NeuroImage 199 (2019) 366–374

Contents lists available at ScienceDirect

NeuroImage

journal homepage: www.elsevier.com/locate/neuroimage

Quantitatively validating the efficacy of artifact suppression techniques to study the cortical consequences of deep brain stimulation with magnetoencephalography

Matthew J. Boring [a,b,c,*], Zachary F. Jessen [d], Thomas A. Wozny [c], Michael J. Ward [c], Ashley C. Whiteman [c], R. Mark Richardson [a,b,c], Avniel Singh Ghuman [a,b,c]

[a] Center for Neuroscience at the University of Pittsburgh, University of Pittsburgh, Pittsburgh, PA, USA
[b] Center for the Neural Basis of Cognition, University of Pittsburgh and Carnegie Mellon University, Pittsburgh, PA, USA
[c] Department of Neurological Surgery, University of Pittsburgh, Pittsburgh, PA, USA
[d] Medical Scientist Training Program, Northwestern University, Chicago, IL, USA

ARTICLE INFO

Keywords:
Magnetoencephalography
Deep brain stimulation
Multivariate pattern analysis
Preprocessing
Temporal signal space separation
Parkinson's disease
Movement disorders

ABSTRACT

Deep brain stimulation (DBS) is an established and effective treatment for several movement disorders and is being developed to treat a host of neuropsychiatric disorders including epilepsy, chronic pain, obsessive compulsive disorder, and depression. However, the neural mechanisms through which DBS produces therapeutic benefits, and in some cases unwanted side effects, in these disorders are only partially understood. Non-invasive neuroimaging techniques that can assess the neural effects of active stimulation are important for advancing our understanding of the neural basis of DBS therapy. Magnetoencephalography (MEG) is a safe, passive imaging modality with relatively high spatiotemporal resolution, which makes it a potentially powerful method for examining the cortical network effects of DBS. However, the degree to which magnetic artifacts produced by stimulation and the associated hardware can be suppressed from MEG data, and the comparability between signals measured during DBS-on and DBS-off conditions, have not been fully quantified. The present study used machine learning methods in conjunction with a visual perception task, which should be relatively unaffected by DBS, to quantify how well neural data can be salvaged from artifact contamination introduced by DBS and how comparable DBS-on and DBS-off data are after artifact removal. Machine learning also allowed us to determine whether the spatiotemporal pattern of neural activity recorded during stimulation are comparable to those recorded when stimulation is off. The spatiotemporal patterns of visually evoked neural fields could be accurately classified in all 8 patients with DBS implants during both DBS-on and DBS-off conditions and performed comparably across those two conditions. Further, the classification accuracy for classifiers trained on the spatiotemporal patterns evoked during DBS-on trials and applied to DBS-off trials, and vice versa, were similar to that of the classifiers trained and tested on either trial type, demonstrating the comparability of these patterns across conditions. Together, these results demonstrate the ability of MEG preprocessing techniques, like temporal signal space separation, to salvage neural data from recordings contaminated with DBS artifacts and validate MEG as a powerful tool to study the cortical consequences of DBS.

1. Introduction

Over the past several decades, deep brain stimulation [DBS] has emerged as an increasingly common treatment option for Parkinson's disease and other movement disorders (Coubes et al., 2004; Limousin et al., 1998; Miocinovic et al., 2013). Additionally, it is being investigated as a potential treatment for neuropsychiatric disorders such as chronic pain (Pereira and Aziz, 2014), obsessive compulsive disorder (Mallet et al., 2008), Tourette's Syndrome (Ackermans et al., 2011), addiction (Alba-Ferrara et al., 2014), Alzheimer's disease (Laxton et al., 2010), and depression (Holtzheimer et al., 2012). Despite its increasing prevalence, the mechanisms whereby DBS produces therapeutic outcomes and unwanted side effects in these disorders are largely unknown (Alhourani et al., 2015). This is partially due to limitations in the ability to

* Corresponding author. 3550 Terrace St., S906 Scaife Hall, Pittsburgh, PA, 15213, USA.
E-mail address: mjb200@pitt.edu (M.J. Boring).

https://doi.org/10.1016/j.neuroimage.2019.05.080
Received 20 March 2019; Received in revised form 16 May 2019; Accepted 29 May 2019
Available online 31 May 2019

non-invasively examine dynamic neural activity evoked by DBS, which requires comparisons between neural activity when the DBS device is on versus when it is off. These comparisons remain challenging because meaningful changes in neural activity must be isolated from signal artifacts introduced by DBS and the associated hardware.

Positron emission tomography [PET], functional magnetic resonance imaging [fMRI], and electroencephalography [EEG] have all been employed to investigate the therapeutic effects of DBS on different diseases [see (Alhourani et al., 2015; Hamani and Moro, 2012; Perlmutter and Mink, 2006) for review]. However, all have inherent limitations, which make them imperfect for investigating this question. For example, hemodynamic responses measured with PET and fMRI lack the temporal resolution necessary to examine altered oscillatory dynamics evoked by DBS. In addition to this, the safety of exposing DBS subjects to the large magnetic fields produced by fMRI has been previously called into question (Finelli et al., 2002; Georgi et al., 2004; Shrivastava et al., 2012), despite some evidence that it is safe (Carmichael et al., 2007). EEG lacks the spatial resolution to accurately localize the downstream effects of DBS and is highly contaminated by electrical artifacts produced by stimulation.

Magnetoencephalography (MEG), on the other hand, is a particularly suitable approach to studying the effects of DBS stimulation (Harmsen et al., 2018). MEG is a passive imaging modality which does not introduce any safety concerns to DBS patients, even with ferromagnetic implants. However, MEG is susceptible to magnetic artifacts caused by DBS (Airaksinen et al., 2011) and those produced by the movement of DBS extension wires extending from the implant to battery pack (Airaksinen et al., 2011; Litvak et al., 2010). Despite this, several studies have suggested that various artifact rejection methods like temporal signal space separation [tSSS] (Taulu and Hari, 2009; Taulu and Simola, 2006), independent component analysis (Abbasi et al., 2016) and null beamforming (Litvak et al., 2010; Mohseni et al., 2012, 2010) have been proposed for suppressing these artifacts and salvaging physiologically relevant brain information (Airaksinen et al., 2011; Gopalakrishnan et al., 2018; Kringelbach et al., 2007; Litvak et al., 2010; Mäkelä et al., 2007; Mohseni et al., 2010; Park et al., 2009). And unlike PET, fMRI, and EEG, MEG signals have spatiotemporal fidelity and provide information from the entire brain, which makes it potentially very useful for investigating how DBS effects distributed cortical processing networks.

Although several studies have shown the utility of various artifact rejection techniques, analysis of MEG-DBS data remains difficult due to persistence of magnetic artifacts in the data (Cao et al., 2017, 2015; Mäkelä et al., 2007), or loss of physiological signal to noise due to cross-contamination of artifact with meaningful brain signal (Abbasi et al., 2016). Therefore, MEG-DBS recordings require careful analysis of the affected frequency ranges (Cao et al., 2015) and currently resorts to qualitative judgements as to which signal aspects are physiological versus artifact. In particular, quantification of the similarity of neural signal acquired during DBS (DBS-on) and when the DBS stimulator is off (DBS-off) using MEG after artifact rejection has not been done to confirm the utility of various artifact rejection techniques. Previous work examining artifact suppression in MEG has largely relied on paradigms that may be affected by DBS, like motor tasks or resting state. This makes comparisons of artifact suppression between DBS-on and DBS-off difficult because it is ambiguous whether differences seen between those conditions are due to differences in neural activity between conditions or differences in residual artifact. It is critical to examine if the neural signals are comparable across the DBS-on and DBS-off conditions for a task that should be relatively unaffected by the stimulation to ensure that differences are not due to differences in the residual artifact. Studies that have investigated the comparability between DBS-on and DBS-off MEG data in a paradigm that was not expected to be affected by DBS stimulation, like visual stimulation, did not quantitatively assess the similarity between signals obtained in the two conditions (Abbasi et al., 2016). These quantitative analyses are necessary to confirm the utility of MEG for studying the neural basis of therapeutic effects and side effects of DBS.

The aim of this study was to quantitatively assess MEG data collected from patients with DBS implants for the treatment of Parkinson's disease during a visual categorization paradigm. Because previous studies have demonstrated that object recognition is intact in movement disorders (Weil et al., 2016), even in advanced Parkinson's with visual hallucinations (Meppelink et al., 2008), it is likely that the neural responses evoked during this task are not be influenced by DBS. Statistical machine-learning was used to classify the spatiotemporal patterns of visually evoked fields in MEG sensor space acquired during DBS-on and DBS-off conditions. Machine learning allows us to quantitatively compare the degree to which spatiotemporal patterns of neural activity were resistant to DBS associated artifacts and artifact suppression techniques across these conditions on a single trial basis without relying on qualitative judgements. By comparing the time-course of classification between DBS-on and DBS-off, as well as applying a classifier trained on the spatiotemporal activity evoked during DBS-on trials to classify the spatiotemporal activity evoked during DBS-off trials and vice versa, we can quantify the spatiotemporal similarity of DBS-on versus DBS-off conditions for a task that should be unaffected by DBS. Also, by applying the same technique to data acquired from healthy controls without DBS implants we can assess if classification performance is similar to a normative population.

Signal processing techniques like SSP, band-pass filtering, tSSS, and dimensionality reduction with principal component analysis greatly improved the accuracy of classifiers in both the DBS-on and DBS-off conditions. These preprocessing techniques were chosen for evaluation due to their ease of implementation and reported efficacy (Gross et al., 2013). The performance of classifiers trained to categorize trials of different visual-object categories in both the DBS-on and off conditions was similar to that of classifiers trained on data from healthy controls. This suggests that, with artifact rejection, physiologically relevant MEG data can be salvaged from DBS artifacts. Further, classifiers trained on the spatiotemporal patterns evoked during trials from the DBS-on condition and tested on the DBS-off condition and vice versa performed comparably to those trained and tested on the same trial condition. This suggests that the spatiotemporal neural signatures of visual-object perception are highly similar across DBS-on and DBS-off conditions after artifact suppression. These results provide quantitative evidence that signal processing techniques are effective at salvaging physiologically relevant MEG signals and confirms that MEG is a reliable and potentially powerful modality for investigation of whole-brain effects of DBS.

2. Methods

2.1. Subjects

Subjects were eight patients with bilateral DBS implants for the treatment of Parkinson's disease, and 9 healthy controls all of which gave informed consent to participate under protocols approved by the University of Pittsburgh Institutional Review Board. Demographic information and stimulation parameters of patients are presented in Table 1. All subjects had implants in either the subthalamic nucleus (STN) or globus pallidus internus (GPi). Stimulation parameters are bilateral unless denoted with left (L) and right (R) designations. Healthy controls were 6 females and 4 males from 19 to 36 years old.

2.2. Experimental paradigm

Eight patients with bilateral DBS implants for the treatment of Parkinson's disease were seated upright and presented with pictures of faces, words, houses, and phase-scrambled faces via a screen 1 m in front of them. Stimuli occupied approximately $10 \times 10^{\circ}$ of visual angle and were delivered via custom scripted Psychtoolbox code (Brainard, 1997). Stimuli were shown for 900 ms with a random 1.5–1.9 s inter-trial interval. Patients were asked to respond if an image was presented twice in a row, which occurred with a probability of 1/10. These repeat trials

Table 1
Patient demographic information.

Patient ID	Age	Gender	Handed-ness	Location	Stimulation Frequency	Voltage	Pulse Width
P1	61	M	R	STN	180Hz	(L) 3.3 V, (R) 2.7 V	(L) 60 μs (R) 90 μs
P2	72	F	R	STN	130Hz	(L) 2.4 V, (R) 1.6 V	60 μs
P3	78	M	R	STN	160 Hz	(L) 1.0 V, (R) 2.8 V	60 μs
P4	67	M	L	STN	160 Hz	(L) 1.5 V, (R) 1.7 V	60 μs
P5	69	M	R	GPi	130 Hz	(L) 2.9 V, (R) 3.0 V	60 μs
P6	71	M	R	STN	160 Hz	(L) 3.4 V, (R) 0.0 V	60 μs
P7	69	F	R	STN	130 Hz	(L) 2.1 V, (R) 2.1 V	60 μs
P8	61	M	R	STN	160 Hz	(L) 4.3 V, (R) 1.9 V	60 μs

were not included in the subsequent analysis. Four blocks of trials were conducted with DBS-on then four blocks of trials with DBS-off yielded 120 trials per stimulus category for both conditions.

To compare results obtained from patients with DBS implants to healthy controls, we ran similar analyses on data collected from 9 healthy controls for the purpose of a different experiment (unpublished). The experimental paradigm was similar across patients and controls except that healthy controls viewed pictures of faces, hammers, houses, and phase-scrambled faces which repeated twice in a row 1/6 of the time. The task was broken into three blocks yielding the same number of stimulus repetitions per category and stimuli were only left on the screen for 300 ms. Longer stimulus presentation was used for DBS patients because they found 300 ms to be too fast.

2.3. Data collection and preprocessing

Data were collected from 204 gradiometers and 102 magnetometers arranged in orthogonal triplets on an Elekta Neuromag Vectorview MEG system (Elekta Oy, Helsinki, Finland). Data were sampled at 1000 Hz. Head position indicators were used to continuously monitor head position during MEG data acquisition.

MEG data preprocessing steps were chosen due to their ease of implementation and reported efficacy (Gross et al., 2013), while achieving robust artifact suppression. Signal-space projection (SSP) (Tesche et al., 1995; Uusitalo and Ilmoniemi, 1997) was performed on MEG data using operators that were tailored based on empty room data to eliminate environmental artifacts. Data were subsequently band-pass filtered from 1 to 50 Hz using default MNE-C filter parameters: 5 Hz low-pass transition band, 3-sample high-pass transition band, and 8917 sample filter length (Gramfort et al., 2014). Subsequently, data were down-sampled to 250 Hz, then processed via temporal signal space separation [tSSS] (Taulu and Hari, 2009; Taulu and Simola, 2006) using Elekta's MaxFilter software (Elekta Oy, Helsinki, Finland), with 10-s buffer length and correlation limit of 0.98. Data was then epoched into 1500 ms trials from −250 to 1250 ms around stimulus presentation. Fig. 1 illustrates this processing pipeline. Performance of multivariate classifiers applied to each of these preprocessing stages is presented in *Results*.

2.4. Multivariate spatio-temporal pattern analysis

Multivariate spatio-temporal pattern analysis was used to assess the amount of information regarding stimulus identity was contained within the stimulus evoked magnetic fields. Multivariate classification methods have been shown to be more sensitive to these stimulus evoked changes than classical univariate methods, because they integrate information across many sensors and timepoints unlike univariate methods (Haxby et al., 2014). This technique was applied to the 306 MEG sensors at 100 ms sliding time windows with a time-step of 12 ms.

Specifically, data was first partitioned for 3-fold cross-validation to ensure independent training and testing of the classifiers, this low number of cross-folds was chosen because visually-evoked categorical information has been shown to be robust in healthy controls (Cichy et al., 2014), therefore a relatively small training set should be sufficient to capture these statistical regularities. A higher number of cross-folds, which would allow for higher number of training trials at the expense of computation time, was not necessary. In analyses involving principle-component analysis (PCA), this procedure was applied to the entire time-course of training data to reduce the effective number of sensors and produce orthogonal components explaining 99% of the total variance. This procedure reduces the dimensionality of the data which helps reduce over-fitting of the classifiers (Hughes, 1968) and can help suppress small sources of noise. PCA was applied independently during each training cross-fold and participant. Therefore, it is not assumed that the PCA coefficients are stable across participants.

Four-way L2-regularized logistic regression was then applied independently to each 100 ms time window via LIBLINEAR (Fan et al., 2008). All results are reported in terms of the first time-point of this 100 ms window. This particular classifier was chosen because logistic regression is relatively simple to employ in future studies and L2-regularization of this classifier helps prevent data overfitting by favoring feature weights that are close to zero (Ng, 2004). The goal of the classifier is to predict which stimulus category (face, word, house or phase-scrambled face) the participant is viewing given the spatiotemporal MEG data. Since each category was presented an equal number of times, random guesses would result in a chance accuracy of 25%. The average decoding accuracy across these three folds are reported across time. Cross-decoding analyses involve predicting stimulus categories learned using data solely from trials where the DBS stimulator is on and applying that to trials where the DBS stimulator is off and vice versa. In these analyses the data was not

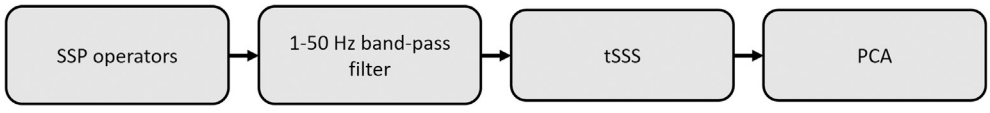

Fig. 1. MEG preprocessing pipeline. Data collected during trials with DBS stimulation and without DBS stimulation were preprocessed using SSP, 1–50 Hz band-pass filters and tSSS. After each step, multivariate pattern analysis was used to determine the amount of visually evoked information could be extracted from the signal. After applying tSSS, the additional utility of PCA was tested to determine if dimensionality reduction improved classification accuracy. Data collected from healthy controls were preprocessed identically.

partitioned into cross-folds.

2.5. Statistics

Above chance classification performance across patients or healthy controls was determined using nonparametric permutation tests (Maris and Oostenveld, 2007). This procedure involved subtracting the chance classification accuracy (25%) then randomly flipping the sign of a subset of participant classification time courses. Next, a *t*-test was performed to compare the permuted group accuracy to zero. T-statistics of clusters of timepoints with an uncorrected p-value less than 0.01 were summed over (cluster forming threshold). Minimum and maximum cluster t-values were stored for all possible combinations of sign flips and compared to those derived from the true classification time courses to calculate corrected p-values.

Difference in classification accuracy between DBS-on versus DBS-off conditions was also determined via non-parametric permutation tests. Classification time course condition labels (DBS-on versus DBS-off) were randomly assigned for each subject and a *t*-test was performed across subjects to compute the difference in permuted time courses. T-statistics of clusters of timepoints with an uncorrected p-value less than 0.01 were summed over (cluster forming threshold). Minimum and maximum cluster t-values were stored for all possible combinations of sign flips and compared to those derived from the true comparison of DBS-on versus off classification time courses to calculate corrected p-values.

Above chance classification accuracy for individual patients was determined by randomly shuffling category labels 1,000,000 times and performing random guess classification. This allowed us to determine a global null distribution from which we calculated the $p < 0.001$ uncorrected chance level, or $p < 0.05$ Bonferroni corrected chance level for both classification accuracy and d' sensitivity. Finally, to compare the difference of peak classification accuracy across different levels of preprocessing, paired *t*-test were conducted for the peak accuracies with Bonferroni correction of p-values across multiple temporal comparisons.

3. Results

L2-regularized logistic regression was used to determine the fidelity of category-specific MEG signals evoked by pictures of words, faces, houses and phase-scrambled faces during active DBS stimulation (DBS-on) and while the stimulator was inactive (DBS-off). Four-way classifiers were used to predict category-level visual information after applying artifact rejection techniques including signal-space projection (SSP), band-pass filtering, temporal signal space separation [tSSS] and dimensionality reduction with principal component analysis (PCA). Above-chance decoding accuracy at the cluster level was not obtained when training classifiers on data preprocessed with only SSP to remove sources of environmental noise in the shielded room (DBS-on max mean±standard error: 28.49±2.1% at 260 ms, DBS-off max mean±standard error: 27.93±0.93% at 236 ms). However, after band pass filtering the MEG data from 1 to 50 Hz there was a modest ability to decode the four object categories (DBS-on max mean±standard error: 44.69±5.83% at 212 ms, DBS-off max mean±standard error: 36.34±2.87% at 200 ms; Fig. 2A and B, respectively). Timepoints between from 152 to 248 ms were significant at the cluster level for DBS-off data ($p < 0.05$). Although DBS-on decoding tended to be more accurate on average, there was no significant difference between the decoding accuracy obtained from DBS-on versus DBS-off trials at the $p < 0.05$ cluster level after processing the data with a 1–50 Hz band-pass filter and SSP (Fig. 3).

Temporal signal space separation (tSSS) applied to the band-pass filtered data improved decoding accuracy in both the DBS-on (max mean±standard error: 64.90±5.82% at 236 ms) and DBS-off conditions (max mean±standard error: 60.07±6.54% at 236 ms; Fig. 2A and B, respectively). Several clusters of time points from 100 to 650 ms were classified significantly above chance for both DBS-on and DBS-off trials. The decoding accuracy obtained on tSSS preprocessed data relative to that obtained from data processed with only a 1–50 Hz band-pass filter and SSP was not statistically significant at the Bonferroni corrected level. However, this relationship was trending (DBS-on: $t(7) > 2.90$, $p < 0.01$, uncorrected from 164 to 344 ms, DBS-off: $t(7) > 3.62$, $p < 0.01$, uncorrected from 104 to 308 ms). At this level of preprocessing, a cluster of timepoints from 1112 to 1136 ms was significantly different between DBS-on and DBS-off trials at the $p < 0.05$ cluster level (Fig. 3).

Dimensionality reduction of the tSSS preprocessed MEG sensor data with PCA further improved classification accuracy in both the DBS-on (max mean±standard error: 71.20±6.61% at 236 ms) and DBS-off conditions (max mean±standard error: 66.48±7.33% at 224 ms; Fig. 2A and B, respectively). For DBS-on and DBS-off trials, this was not a significant improvement in peak classification relative to trials processed with SSP, 1–50 Hz band-pass filter, and tSSS. Testing individual subject decoding accuracies at this level of preprocessing revealed decoding accuracies above chance at the $p < 0.05$, Bonferroni corrected level for all eight subjects in both DBS-on and DBS-off trials (Fig. 4). After correcting for multiple comparisons in time, there was no significant difference at the

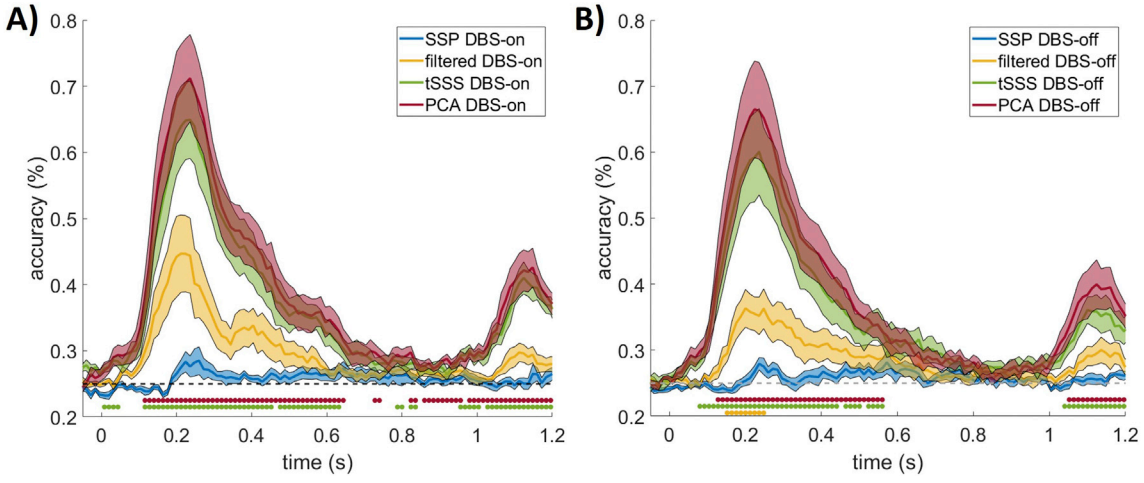

Fig. 2. Average decoding accuracy across all subjects for DBS-on and DBS-off trials at four different levels of preprocessing. Each level of processing includes lower levels, i.e. PCA results were also preprocessed with tSSS, filtering, and SSP. Accuracy is reported at the first time point of the 100 ms sliding window. A) Decoding accuracy across DBS-on trials after applying SSP, band-pass filtering from 1 to 50 Hz, applying tSSS, and reducing the data dimensionality with PCA. Clusters of timepoints with above chance classification accuracy ($p < 0.05$, corrected) are indicated below each curve. Error bars represent standard error across subjects. B) Decoding accuracy across DBS-off trials for the same four levels of preprocessing.

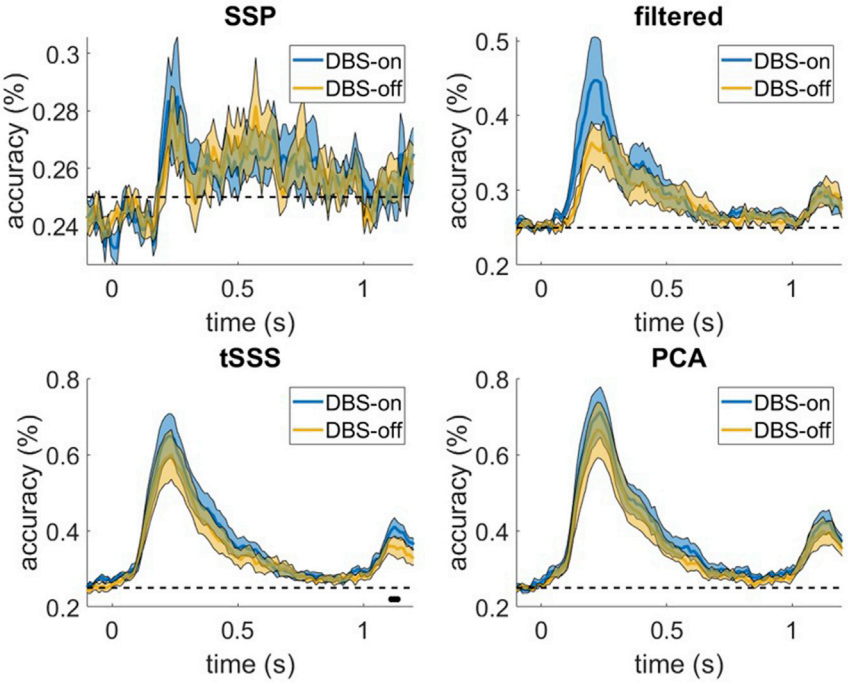

Fig. 3. Average decoding accuracy across patients during DBS-on and DBS-off trials at each preprocessing level. Each level of processing includes lower levels, i.e. PCA results were also preprocessed with tSSS, filtering, and SSP. Curves are identical to those in Fig. 2 but pictured to allow for easier comparison across DBS-on and DBS-off conditions. Black dots under the curves indicate clusters of timepoints that are significantly different across the two conditions ($p < 0.05$, corrected). Error bars represent standard error across subjects. The only significant cluster was found after preprocessing with tSSS from 1112 to 1136 ms, during which DBS-on trials were classified more reliably than DBS-off trials.

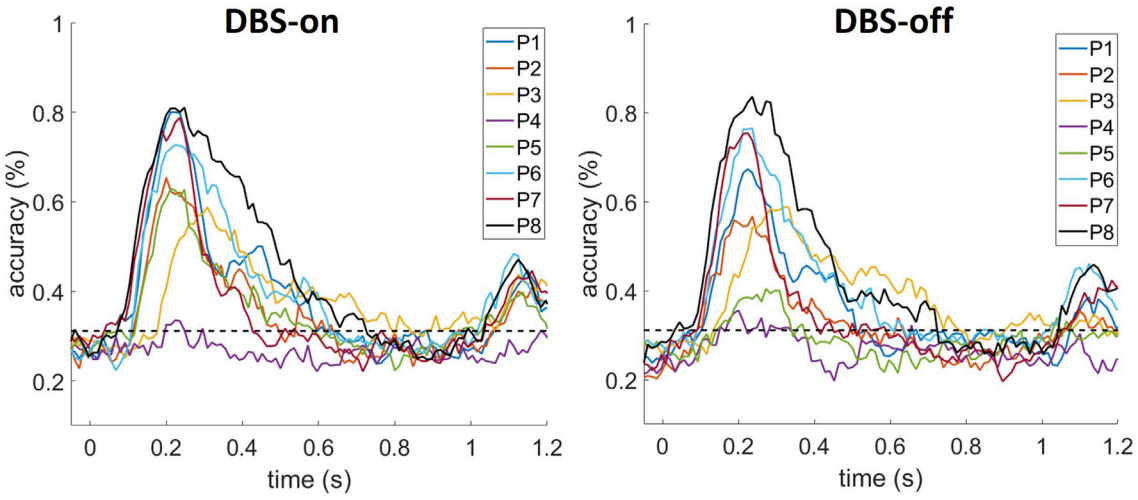

Fig. 4. Decoding accuracy of four-way L2 regularized logistic regression classifier for all eight participants in both DBS-on and DBS-off blocks. Data was preprocessed with SSP, 1–50 Hz band-pass filter, tSSS, and PCA. Grey dotted line represents Bonferroni corrected threshold for $p < 0.05$ four-way decoding accuracy.

cluster level between DBS-on versus DBS-off trials at this level of processing although DBS-on trials were classified slightly more reliably (Fig. 3). Because tSSS in combination with PCA performed the best, all further analyses were conducted at this level of preprocessing.

To compare the amount of physiologically relevant brain information contained in the MEG data across patients with DBS implants and healthy controls we ran the same preprocessing pipeline on healthy control data collected from a similar experiment (see *Methods*). Classification accuracy during the first 300 ms of the trial, when the stimulus was present in both DBS and healthy control paradigms, was not significantly different from one another (Fig. 5B). However, decoding of healthy control data from 524 to 584 ms was significantly greater than decoding of DBS patient data ($p < 0.05$, corrected), which we speculate is due to the response to the offset of the stimulus in the healthy control paradigm that did not coincide with the offset of the stimulus in the DBS paradigm (300 ms offset in the healthy controls, 900 ms offset in DBS). A similar difference manifested at the offset of the stimulus in the DBS patient experiment, where DBS patient data was classified with significantly higher accuracy than healthy control data from 1028 ms to 1232 ms ($p < 0.01$, corrected). To determine if data collected from healthy controls benefitted from artifact suppression with tSSS like the data collected from DBS patients, we compared the decoding time course of healthy control data at each step of the preprocessing (Fig. 6). Filtering the healthy control data greatly improved decoding accuracy, whereas the remaining preprocessing steps did not significantly improve decoding accuracy, unlike the DBS data (Fig. 2). The sharp rise for the unfiltered data around 100 ms versus the more gradual and earlier rise in the filtered data are likely to be artifacts of using a non-causal filter for the band pass; e.g. the shallow rise in decoding accuracy prior to 100 ms in the filtered, tSSS, and PCA results is not likely to be a result of improved sensitivity and instead is likely a result of a filter artifact that could be overcome by using a causal filter or lower high pass threshold (Acunzo

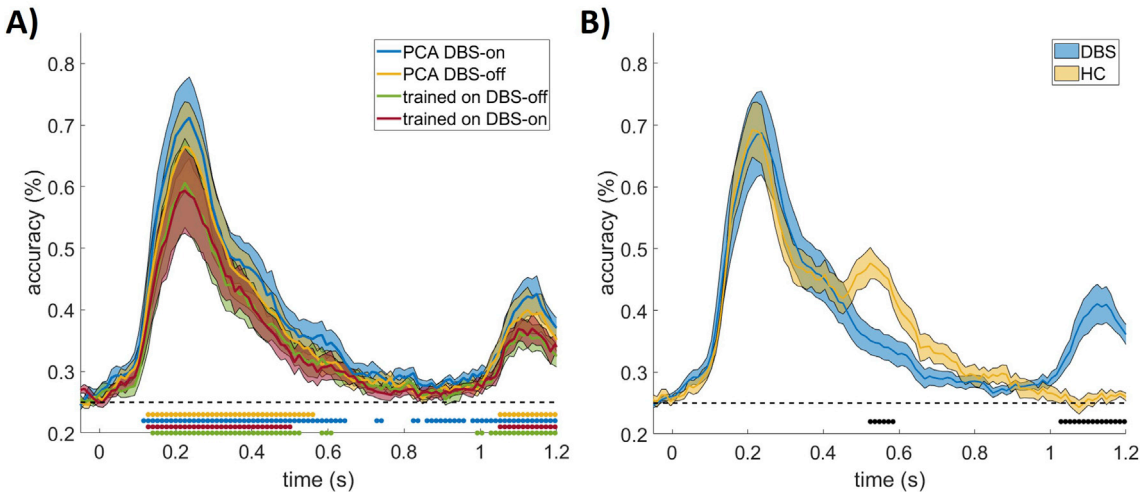

Fig. 5. Decoding preprocessed MEG signals from DBS patients and healthy controls. A) Decoding accuracy for data preprocessed at the highest level (SSP, 1–50 Hz band-pass filter, tSSS, and PCA) across DBS-on, DBS-off, and cross-decoding. Cross-decoding refers to training a classifier solely on data collected from the DBS-on trials than testing on the DBS-off trials (trained on DBS-on) and vice-versa (trained on DBS-off). Clusters of timepoints with above chance classification accuracy ($p < 0.05$, corrected) are indicated below each curve. Error bars represent standard error across subjects. B) Average decoding of DBS-on and DBS-off trials compared with that of healthy controls. Clusters of timepoints significantly different between the curves ($p < 0.05$, corrected) are indicated with black dots. Stimuli were removed from the screen at 300 ms in controls but left on for 900 ms in DBS patients for their comfort (see *Methods*). The second peaks of decoding across the groups are likely to be the offset response and therefore different due to the different image removal times.

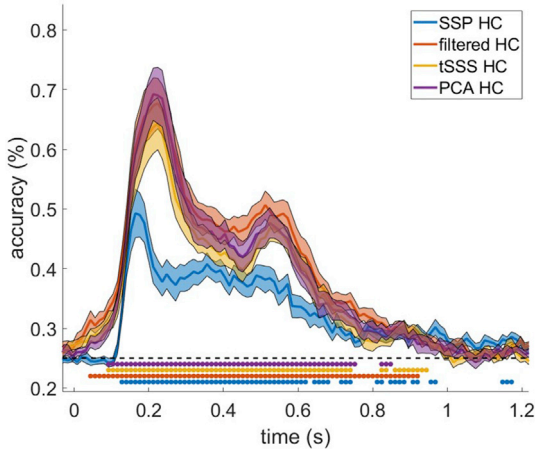

Fig. 6. Average decoding accuracy of healthy control data preprocessed with the same pipeline as the DBS patient data (Fig. 2). Each level of processing includes lower levels, i.e. PCA results were also preprocessed with tSSS, filtering, and SSP. Accuracy is reported at the first time point of the 100 ms sliding window. Clusters of timepoints with above chance classification accuracy ($p < 0.05$, corrected) are indicated below each curve. Error bars represent standard error across subjects.

et al., 2012; Rousselet, 2012).

Next, to assess the similarity between the spatiotemporal patterns evoked from the visual object categories during DBS-on and DBS-off trials, classifiers were trained on the spatiotemporal patterns of MEG sensor data evoked during DBS-on trials and tested on DBS-off trials and vice versa. These classifiers also performed significantly above chance (max mean±standard error: 60.07±6.07% at 224 ms for classifiers trained on DBS-off data and max mean±standard error: 59.27±6.91% at 224 ms for classifiers trained on DBS-on data, Fig. 5A). Notably, this decoding accuracy was not significantly different from those derived from DBS-off trials at the $p < 0.05$ cluster corrected level, although this relationship was trending ($t(7) > 3.69$, $p < 0.01$, uncorrected from 200 to 248 ms). This shows that, for the most part, spatiotemporal patterns of visually evoked neural activity were preserved across DBS-on versus off trials. This was supported when looking at sensitivity indices of all object categories in the DBS-on versus DBS-off conditions (Fig. 7). Across DBS-on and DBS-off classifiers, object categories demonstrated very similar relative sensitivities. This conservation of relative decoding among object categories suggests that no one object category was overly affected by DBS-induced artifacts relative to others.

4. Discussion

The results presented here provide quantitative evidence for the utility of MEG preprocessing strategies in removing magnetic artifacts induced by DBS and the associated hardware while sparing dynamic neural activity in tasks that should be unaffected by the stimulation. A combination of band-pass filtering, SSP, tSSS and dimensionality reduction with PCA allowed for the highest classification accuracy, which was above chance for eight out of eight of our tested patients. Further, by demonstrating the generalizability of classifiers trained on the spatiotemporal patterns of MEG data evoked during trials with active DBS and tested on trials where the stimulator was inactive and vice versa, we were able to confirm that the spatiotemporal dynamics of the neural signals was comparable across the DBS-on and DBS-off conditions. Additionally, classification accuracy and time-course were similar between patients with DBS implants and healthy controls.

Without applying any level of signal preprocessing, besides SSP to remove environmental artifacts, reliable decoding accuracy was not obtained with classifiers trained on either DBS-on or DBS-off data. It is possible that the SSP method may be useful for removing DBS artifacts if the SSP operators are updated to specifically tailored to the DBS recordings, however using these operators to just remove environmental noise leaves the signal too contaminated by artifact for accurate classification. After preprocessing with a 1–50 Hz band-pass filter, we were able to achieve modest classification of the visual categories across the group. Therefore, it is likely that band-pass filtering helps suppress the artifactual components of the frequency spectrum that result from the DBS-stimulation and the associated hardware. Next, the application of tSSS, which been previously shown to effectively suppress magnetic artifacts within the limits of the band-pass filter (Mäkelä et al., 2007), especially those associated with movement of the DBS hardware, further increased the performance of our classifiers. The importance of tSSS for

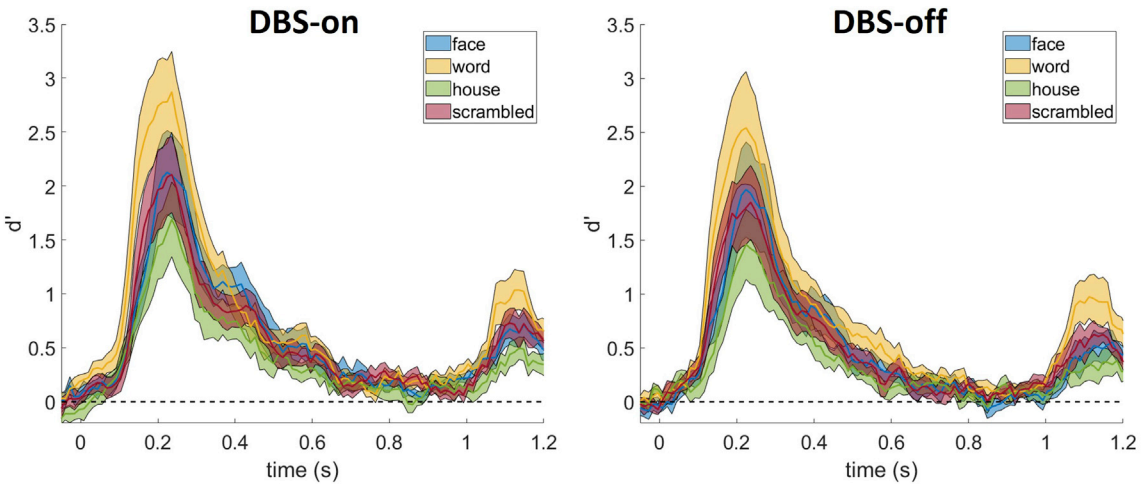

Fig. 7. Average D′ sensitivity for all four object categories across subjects in the category localizer task at highest level of preprocessing (SSP, 1–50 Hz band-pass filter, tSSS, and PCA). Error bars represent standard error from the mean across subjects.

removing the DBS artifact is supported by the fact that data collected from healthy controls achieved similar decoding accuracy before and after preprocessing with tSSS, since there was no DBS hardware associated artifacts in this data, thus it was only beneficial in the presence of DBS artifacts.

Finally, PCA reduces the rich spatiotemporal pattern of the visual response into a lower rank representation by finding orthogonal bases that capture the most variance in the data. These bases are in no way related to their physical significance. Therefore, in order to perform group-level analyses on this data it would have to be projected back through PCA operators into source space, which could then be matched across subjects, or group-level analysis could be done through a multi-set PCA approach to project into a common eigenspace. Given that the visual responses of interest are a large component of the MEG signal, this orthogonal basis faithfully captured this aspect of the signal, while discarding components that capture less of the signal variance, likely reducing noise and classifier over-fitting (Hughes, 1968). This ultimately led to similar classifier performance across DBS patients and healthy control participants, illustrating the efficacy of this combination of preprocessing techniques. In controls, little advantage was seen for tSSS or PCA, suggesting that these may only be useful when unusual artifacts are present, such as those from DBS, and not more broadly useful in the context of MEG decoding studies. Careful analysis of these specific preprocessing stages and their impact on data quality is necessary to ensure their applicability to other types of analysis, i.e. time-frequency decomposition, and cognitive domains, i.e. motor tasks.

We acknowledge that age differences between DBS patients and healthy controls is a potential confound in this analysis, as is the difference in presentation duration of the stimuli. It is possible that similar classification accuracies derived from these groups is the result of interacting effects. DBS-induced detriments to signal quality could be canceled by increased discriminability of the object categories in older relative to younger adults or by longer image presentation times in DBS patients relative to healthy controls. However, the time course of decoding between DBS patients and healthy controls was similar during the first 300 ms of the response when the stimulus was on for both groups. Further, it has been shown using fMRI that ventral visual stream representations of different object categories become more similar to one another with age (Park et al., 2004). Therefore, we consider this explanation unlikely and suggest that the results indicate that, after artifact removal, the data is comparable between controls and patients with DBS artifacts.

Despite the potential applications of MEG in DBS research, one methodological note for future DBS studies using MEG is that the DBS stimulator hardware initially interfered with head position indicator (HPI) coils when the HPI coils were at their default setting across both DBS-on and DBS-off conditions. This made accurate head localization and subsequent source localization impossible. Thus, the frequency of the HPI coils should be adjusted to a frequency that is uninfluenced by the DBS stimulator. Even with this adjustment of the HPI coil frequency, we found that continuous head localization for movement correction was not always possible. In the future, it may be helpful to high pass filter the data to suppress movement related artifacts prior to attempting this correction.

Given that the wires extending from the DBS implant to the battery pack generate large magnetic fields during patient movement, movement artifacts are exacerbated by the DBS hardware. Indeed, the fact that the DBS-on and DBS-off data appear to be similar even before artifact removal suggests that the main artifact in these data are a result of the presence of the DBS hardware, not the stimulation per se. An important potential caveat for studies where head motion, and DBS artifacts that are exacerbated by head motion, is that head movement artifacts may still be an issue even after the artifact removal procedure described here. Therefore, patients which are unable to keep still during the MEG tasks should likely be excluded from studies, which may bias the population of patients that are able to be covered in DBS-MEG studies, particularly for movement disorders research.

In addition to these considerations, it is important for future studies to continue to carefully examine the feasibility of isolating artifactual DBS components from DBS-induced physiological changes. For example, the current study did not address the feasibility of removing response-related movement artifacts from physiological changes in motor related fields, an important next step in realizing MEG's utility for understanding the therapeutic effects of DBS during movement. Although previous studies, including this one, have demonstrated the utility of tSSS for suppressing DBS artifacts induced by respiration or sporadic movements (Airaksinen et al., 2011; Connolly et al., 2012; Mäkelä et al., 2007; Park et al., 2009), it has not been demonstrated in the context where movement is systematically related to the neural response of interest. For example, it remains unclear whether one can compare the event related fields evoked by even small cued motor movements with and without DBS stimulation. Doing so will both be important and challenging because it will be difficult to assess whether any differences between DBS-on and DBS-off are due to neural differences when performing the task or due to residual differences in artifacts that may be accentuated by differences in movement. In addition, the paradigm used here, cross-classification of data for an incidental task, could provide a useful platform for validating and comparing across different artifact removal schemes, for example comparing the pipeline described here to others that have been previously described (Gramfort et al., 2013; Gross et al., 2013).

The results of this study validate MEG as a viable tool to study the cortical consequences of DBS in humans and open up critical new avenues of research for understanding the neuroscientific mechanisms of DBS and for potential clinical and translational work to improve the efficacy of DBS. For example, intraoperative recordings suggest that DBS modulates aberrant spectral power components in the beta frequency range and beta band synchrony between cortical and subcortical motor systems (de Hemptinne et al., 2015; Kondylis et al., 2016). MEG can be used to examine the chronic effects of DBS on cortical beta rhythms both in and outside of the motor system. Resting-state MEG comparing DBS-on with DBS-off can be used to assess connectome-level effects of DBS when analyzed using graph theoretical measures. How these network-level modulations relate to clinically significant therapeutic effects and side effects can inform the development of neural biomarkers for assessing treatment response (e.g. evidence for engagement of the therapeutic target). Using MEG to assess both therapeutic target engagement and the neural correlates of undesirable side effects has the potential to not only inform our understanding of DBS for Parkinson's disease and movement disorders, but also could provide a framework for using MEG as a critical tool in studies aimed at expanding the utility of DBS to other neurological and psychiatric disorders.

One potentially impactful avenue for future research is to use MEG to validate recently developed models which predict the effects of different DBS parameters. These models have been developed using subject-specific anatomical information and DBS localization in conjunction with neurophysiological parameters to estimate the volume of tissue affected, and the cortical regions modulated, by DBS. These models estimate the differential effects expected with different stimulation parameters, such as stimulating different leads on the DBS electrode or stimulating with different frequencies or intensities (Butson et al., 2011; Chaturvedi et al., 2010). MEG can be used to help validate these models and ultimately could lead to a quantitative, evidence-based approach for DBS stimulator programming that is both standardized and personalized.

Given recent evidence for the high sensitivity and fidelity in localizing cognitive effects with MEG (Boring et al., 2018), the results presented here strongly suggest that MEG is a reliable and potentially powerful tool for assessing the cortical neurophysiological effects of DBS on non-motor behaviors, at least in patients without a strong resting tremor. Motor behavior assessments may be feasible if great care is taken to reduce movement, for example by using a custom head cast. In conclusion, this study validates the efficacy of artifact removal algorithms in cleansing MEG data contaminated with DBS artifact and sets the stage for future studies to examine the therapeutic and side effects of DBS.

Declaration of interests

The authors declare no competing interests.

Acknowledgements

The authors would like to thank the subjects and their families for their participation in this research study. This work was supported by the National Institutes of Health (T32NS007433-20 to M.J.B., R01MH107797 and R21MH103592 to A.S.G.) and the Brain & Behavior Research Foundation (NARSAD Young Investigator Grant to R.M.R.).

References

Abbasi, O., Hirschmann, J., Schmitz, G., Schnitzler, A., Butz, M., 2016. Rejecting deep brain stimulation artefacts from MEG data using ICA and mutual information. J. Neurosci. Methods 268, 131–141. https://doi.org/10.1016/J.JNEUMETH.2016.04.010.

Ackermans, L., Duits, A., van der Linden, C., Tijssen, M., Schruers, K., Temel, Y., Kleijer, M., Nederveen, P., Bruggeman, R., Tromp, S., van Kranen-Mastenbroek, V., Kingma, H., Cath, D., Visser-Vandewalle, V., 2011. Double-blind clinical trial of thalamic stimulation in patients with Tourette syndrome. Brain 134, 832–844. https://doi.org/10.1093/brain/awq380.

Acunzo, D.J., MacKenzie, G., van Rossum, M.C.W., 2012. Systematic biases in early ERP and ERF components as a result of high-pass filtering. J. Neurosci. Methods 209, 212–218. https://doi.org/10.1016/j.jneumeth.2012.06.011.

Airaksinen, K., Mäkelä, J.P., Taulu, S., Ahonen, A., Nurminen, J., Schnitzler, A., Pekkonen, E., 2011. Effects of DBS on auditory and somatosensory processing in Parkinson's disease. Hum. Brain Mapp. 32, 1091–1099. https://doi.org/10.1002/hbm.21096.

Alba-Ferrara, L.M., Fernandez, F., de Erausquin, G.A., 2014. The use of neuromodulation in the treatment of cocaine dependence. Addict. Disord. Their Treat. 13, 1–7. https://doi.org/10.1097/ADT.0b013e31827b5a2c.

Alhourani, A., McDowell, M.M., Randazzo, M.J., Wozny, T.A., Kondylis, E.D., Lipski, W.J., Beck, S., Karp, J.F., Ghuman, A.S., Richardson, R.M., 2015. Network effects of deep brain stimulation. J. Neurophysiol. 114, 2105–2117. https://doi.org/10.1152/jn.00275.2015.

Boring, M.J., Hirshorn, E.A., Li, Y., Ward, M.J., Fiez, J.A., Richardson, R.M., Ghuman, A.S., 2018. Top-down and Bottom-Up Interactions Facilitate the Disambiguation of Orthographically Similar Words in the Left Mid-fusiform Gyrus. bioRxiv.

Brainard, D.H., 1997. The psychophysics toolbox. Spatial Vis. 10, 433–436. https://doi.org/10.1163/156856897X00357.

Butson, C.R., Cooper, S.E., Henderson, J.M., Wolgamuth, B., McIntyre, C.C., 2011. Probabilistic analysis of activation volumes generated during deep brain stimulation. Neuroimage 54, 2096–2104. https://doi.org/10.1016/J.NEUROIMAGE.2010.10.059.

Cao, C.-Y., Zeng, K., Li, D.-Y., Zhan, S.-K., Li, X.-L., Sun, B.-M., 2017. Modulations on cortical oscillations by subthalamic deep brain stimulation in patients with Parkinson disease: a MEG study. Neurosci. Lett. 636, 95–100. https://doi.org/10.1016/J.NEULET.2016.11.009.

Cao, C., Li, D., Jiang, T., Ince, N.F., Zhan, S., Zhang, J., Sha, Z., Sun, B., 2015. Resting state cortical oscillations of patients with Parkinson disease and with and without subthalamic deep brain stimulation. J. Clin. Neurophysiol. 32, 109–118. https://doi.org/10.1097/WNP.0000000000000137.

Carmichael, D.W., Pinto, S., Limousin-Dowsey, P., Thobois, S., Allen, P.J., Lemieux, L., Yousry, T., Thornton, J.S., 2007. Functional MRI with active, fully implanted, deep brain stimulation systems: safety and experimental confounds. Neuroimage 37, 508–517. https://doi.org/10.1016/j.neuroimage.2007.04.058.

Chaturvedi, A., Butson, C.R., Lempka, S.F., Cooper, S.E., McIntyre, C.C., 2010. Patient-specific models of deep brain stimulation: influence of field model complexity on neural activation predictions. Brain Stimul 3, 65–77. https://doi.org/10.1016/J.BRS.2010.01.003.

Cichy, R.M., Pantazis, D., Oliva, A., 2014. Resolving human object recognition in space and time. Nat. Neurosci. 17, 455–462. https://doi.org/10.1038/nn.3635.

Connolly, A.T., Bajwa, J.A., Johnson, M.D., 2012. Cortical magnetoencephalography of deep brain stimulation for the treatment of postural tremor. Brain Stimul 5, 616–624. https://doi.org/10.1016/j.brs.2011.11.006.

Coubes, P., Cif, L., El Fertit, H., Hemm, S., Vayssiere, N., Serrat, S., Picot, M.C., Tuffery, S., Claustres, M., Echenne, B., Frerebeau, P., 2004. Electrical stimulation of the globus pallidus internus in patients with primary generalized dystonia: long-term results. J. Neurosurg. 101, 189–194. https://doi.org/10.3171/jns.2004.101.2.0189.

de Hemptinne, C., Swann, N.C., Ostrem, J.L., Ryapolova-Webb, E.S., San Luciano, M., Galifianakis, N.B., Starr, P.A., 2015. Therapeutic deep brain stimulation reduces cortical phase-amplitude coupling in Parkinson's disease. Nat. Neurosci. 18, 779–786. https://doi.org/10.1038/nn.3997.

Fan, R.-E., Chang, K.-W., Hsieh, C.-J., Wang, X.-R., Lin, C.-J., 2008. LIBLINEAR: a library for large linear classification. J. Mach. Learn. Res. 9. http://www.jmlr.org/papers/v9/fan08a.html.

Finelli, D.A., Rezai, A.R., Ruggieri, P.M., Tkach, J.A., Nyenhuis, J.A., Hrdlicka, G., Sharan, A., Gonzalez-Martinez, J., Stypulkowski, P.H., Shellock, F.G., 2002. MR imaging-related heating of deep brain stimulation electrodes: in vitro study. AJNR. Am. J. Neuroradiol. 23, 1795–1802.

Georgi, J.-C., Stippich, C., Tronnier, V.M., Heiland, S., 2004. Active deep brain stimulation during MRI: a feasibility study. Magn. Reson. Med. 51, 380–388. https://doi.org/10.1002/mrm.10699.

Gopalakrishnan, R., Burgess, R.C., Malone, D.A., Lempka, S.F., Gale, J.T., Floden, D.P., Baker, K.B., Machado, A.G., 2018. Deep brain stimulation of the ventral striatal area for poststroke pain syndrome: a magnetoencephalography study. J. Neurophysiol. 119, 2118–2128. https://doi.org/10.1152/jn.00830.2017.

Gramfort, A., Luessi, M., Larson, E., Engemann, D.A., Strohmeier, D., Brodbeck, C., Goj, R., Jas, M., Brooks, T., Parkkonen, L., Hämäläinen, M., 2013. MEG and EEG data analysis with MNE-Python. Front. Neurosci. 7, 267. https://doi.org/10.3389/fnins.2013.00267.

Gramfort, A., Luessi, M., Larson, E., Engemann, D.A., Strohmeier, D., Brodbeck, C., Parkkonen, L., Hämäläinen, M.S., 2014. MNE software for processing MEG and EEG data. Neuroimage 86, 446–460. https://doi.org/10.1016/j.neuroimage.2013.10.027.

Gross, J., Baillet, S., Barnes, G.R., Henson, R.N., Hillebrand, A., Jensen, O., Jerbi, K., Litvak, V., Maess, B., Oostenveld, R., Parkkonen, L., Taylor, J.R., van Wassenhove, V., Wibral, M., Schoffelen, J.-M., 2013. Good practice for conducting and reporting MEG research. Neuroimage 65, 349–363. https://doi.org/10.1016/j.neuroimage.2012.10.001.

Hamani, C., Moro, E., 2012. Emerging horizons in neuromodulation: new frontiers in brain and spine stimulation. Chem. 107, 87–119. https://doi.org/10.1016/B978-0-12-404706-8.09990-3.

Harmsen, I.E., Rowland, N.C., Wennberg, R.A., Lozano, A.M., 2018. Characterizing the effects of deep brain stimulation with magnetoencephalography: a review. Brain Stimul 11, 481–491. https://doi.org/10.1016/J.BRS.2017.12.016.

Haxby, J.V., Connolly, A.C., Guntupalli, J.S., 2014. Decoding Neural Representational Spaces Using Multivariate Pattern Analysis. https://doi.org/10.1146/annurev-neuro-062012-170325.

Holtzheimer, P.E., Kelley, M.E., Gross, R.E., Filkowski, M.M., Garlow, S.J., Barrocas, A., Wint, D., Craighead, M.C., Kozarsky, J., Chismar, R., Moreines, J.L., Mewes, K., Posse, P.R., Gutman, D.A., Mayberg, H.S., 2012. Subcallosal cingulate deep brain stimulation for treatment-resistant unipolar and bipolar depression. Arch. Gen. Psychiatr. 69, 150. https://doi.org/10.1001/archgenpsychiatry.2011.1456.

Hughes, G., 1968. On the mean accuracy of statistical pattern recognizers. IEEE Trans. Inf. Theory 14, 55–63. https://doi.org/10.1109/TIT.1968.1054102.

Kondylis, E.D., Randazzo, M.J., Alhourani, A., Lipski, W.J., Wozny, T.A., Pandya, Y., Ghuman, A.S., Turner, R.S., Crammond, D.J., Richardson, R.M., 2016. Movement-related dynamics of cortical oscillations in Parkinson's disease and essential tremor. Brain 139, 2211–2223. https://doi.org/10.1093/brain/aww144.

Kringelbach, M.L., Jenkinson, N., Green, A.L., Owen, S.L.F., Hansen, P.C., Cornelissen, P.L., Holliday, I.E., Stein, J., Aziz, T.Z., 2007. Deep brain stimulation for chronic pain investigated with magnetoencephalography. Neuroreport 18, 223–228. https://doi.org/10.1097/WNR.0b013e328010dc3d.

Laxton, A.W., Tang-Wai, D.F., McAndrews, M.P., Zumsteg, D., Wennberg, R., Keren, R., Wherrett, J., Naglie, G., Hamani, C., Smith, G.S., Lozano, A.M., 2010. A phase i trial of deep brain stimulation of memory circuits in Alzheimer's disease. Ann. Neurol. 68, 521–534. https://doi.org/10.1002/ana.22089.

Limousin, P., Krack, P., Pollak, P., Benazzouz, A., Ardouin, C., Hoffmann, D., Benabid, A.-L., 1998. Electrical stimulation of the subthalamic nucleus in advanced Parkinson's disease. N. Engl. J. Med. 339, 1105–1111. https://doi.org/10.1056/NEJM199810153391603.

Litvak, V., Eusebio, A., Jha, A., Oostenveld, R., Barnes, G.R., Penny, W.D., Zrinzo, L., Hariz, M.I., Limousin, P., Friston, K.J., Brown, P., 2010. Optimized beamforming for simultaneous MEG and intracranial local field potential recordings in deep brain stimulation patients. Neuroimage 50, 1578–1588. https://doi.org/10.1016/j.neuroimage.2009.12.115.

Mäkelä, J.P., Taulu, S., Pohjola, J., Ahonen, A., Pekkonen, E., 2007. Effects of subthalamic nucleus stimulation on spontaneous sensorimotor MEG activity in a Parkinsonian patient. Int. Congr. Ser. 1300, 345–348. https://doi.org/10.1016/j.ics.2007.02.003.

Mallet, L., Polosan, M., Jaafari, N., Baup, N., Welter, M.-L., Fontaine, D., Montcel, S.T. du, Yelnik, J., Chéreau, I., Arbus, C., Raoul, S., Aouizerate, B., Damier, P., Chabardès, S., Czernecki, V., Ardouin, C., Krebs, M.-O., Bardinet, E., Chaynes, P., Burbaud, P., Cornu, P., Derost, P., Bougerol, T., Bataille, B., Mattei, V., Dormont, D., Devaux, B., Vérin, M., Houeto, J.-L., Pollak, P., Benabid, A.-L., Agid, Y., Krack, P., Millet, B., Pelissolo, A., 2008. Subthalamic nucleus stimulation in severe obsessive–compulsive disorder. N. Engl. J. Med. 359, 2121–2134. https://doi.org/10.1056/NEJMoa0708514.

Maris, E., Oostenveld, R., 2007. Nonparametric statistical testing of EEG- and MEG-data. J. Neurosci. Methods 164, 177–190. https://doi.org/10.1016/J.JNEUMETH.2007.03.024.

Meppelink, A.M., Koerts, J., Borg, M., Leenders, K.L., van Laar, T., 2008. Visual object recognition and attention in Parkinson's disease patients with visual hallucinations. Mov. Disord. 23, 1906–1912. https://doi.org/10.1002/mds.22270.

Miocinovic, S., Somayajula, S., Chitnis, S., Vitek, J.L., 2013. History, applications, and mechanisms of deep brain stimulation. JAMA Neurol 70, 163. https://doi.org/10.1001/2013.jamaneurol.45.

Mohseni, H.R., Kringelbach, M.L., Smith, P.P., Green, A.L., Parsons, C.E., Young, K.S., Brittain, J.-S., Hyam, J.A., Schweder, P.M., Stein, J.F., Aziz, T.Z., 2010. Application of a null-beamformer to source localisation in MEG data of deep brain stimulation. In: 2010 Annual International Conference of the IEEE Engineering in Medicine and Biology. IEEE, pp. 4120–4123. https://doi.org/10.1109/IEMBS.2010.5627325.

Mohseni, H.R., Smith, P.P., Parsons, C.E., Young, K.S., Hyam, J.A., Stein, A., Stein, J.F., Green, A.L., Aziz, T.Z., Kringelbach, M.L., 2012. MEG can map short and long-term changes in brain activity following deep brain stimulation for chronic pain. PLoS One 7, e37993. https://doi.org/10.1371/journal.pone.0037993.

Ng, A.Y., 2004. Feature Selection, L 1 vs. L 2 Regularization, and Rotational Invariance, p. 78. https://doi.org/10.1145/1015330.1015435.

Park, D.C., Polk, T.A., Park, R., Minear, M., Savage, A., Smith, M.R., 2004. Aging reduces neural specialization in ventral visual cortex. Proc. Natl. Acad. Sci. U. S. A 101, 13091–13095. https://doi.org/10.1073/pnas.0405148101.

Park, H., Kim, J.S., Paek, S.H., Jeon, B.S., Lee, J.Y., Chung, C.K., 2009. Cortico-muscular coherence increases with tremor improvement after deep brain stimulation in Parkinson's disease. Neuroreport 20, 1444–1449. https://doi.org/10.1097/WNR.0b013e328331a51a.

Pereira, E.A.C., Aziz, T.Z., 2014. Neuropathic pain and deep brain stimulation. Neurotherapeutics 11, 496–507. https://doi.org/10.1007/s13311-014-0278-x.

Perlmutter, J.S., Mink, J.W., 2006. Deep brain stimulation. Annu. Rev. Neurosci. 29, 229–257. https://doi.org/10.1146/annurev.neuro.29.051605.112824.

Rousselet, G.A., 2012. Does filtering preclude us from studying ERP time-courses? Front. Psychol. 3, 131. https://doi.org/10.3389/fpsyg.2012.00131.

Shrivastava, D., Abosch, A., Hughes, J., Goerke, U., DelaBarre, L., Visaria, R., Harel, N., Vaughan, J.T., 2012. Heating induced near deep brain stimulation lead electrodes during magnetic resonance imaging with a 3 T transceive volume head coil. Phys. Med. Biol. 57, 5651–5665. https://doi.org/10.1088/0031-9155/57/17/5651.

Taulu, S., Hari, R., 2009. Removal of magnetoencephalographic artifacts with temporal signal-space separation: demonstration with single-trial auditory-evoked responses. Hum. Brain Mapp. 30, 1524–1534. https://doi.org/10.1002/hbm.20627.

Taulu, S., Simola, J., 2006. Spatiotemporal signal space separation method for rejecting nearby interference in MEG measurements. Phys. Med. Biol. 51, 1759–1768. https://doi.org/10.1088/0031-9155/51/7/008.

Tesche, C.D., Uusitalo, M.A., Ilmoniemi, R.J., Huotilainen, M., Kajola, M., Salonen, O., 1995. Signal-space projections of MEG data characterize both distributed and well-localized neuronal sources. Electroencephalogr. Clin. Neurophysiol. 95, 189–200. https://doi.org/10.1016/0013-4694(95)00064-6.

Uusitalo, M.A., Ilmoniemi, R.J., 1997. Signal-space projection method for separating MEG or EEG into components. Med. Biol. Eng. Comput. 35, 135–140. https://doi.org/10.1007/BF02534144.

Weil, R.S., Schrag, A.E., Warren, J.D., Crutch, S.J., Lees, A.J., Morris, H.R., 2016. Visual dysfunction in Parkinson's disease. Brain 139, 2827–2843. https://doi.org/10.1093/brain/aww175.